

Ultra-fast All-optical Packet-switched Routing with a Hybrid Header Address Correlation Scheme

M. F. Chiang¹, Z. Ghassemlooy¹, W. P. Ng¹, H. Le Minh², and C. Lu³

¹ Optical Communications Research Group
School of Computing, Engineering and Information Sciences
Northumbria University, Newcastle upon Tyne, UK

Email: ming-feng.chiang@unn.ac.uk, fary.ghassemlooy@unn.ac.uk,
wai-pang.ng@unn.ac.uk,

² Department of Engineering Science, University of Oxford, Oxford, UK
Hoa.le-minh@eng.ox.ac.uk

³ Department of Electronic and Information Engineering
Hong Kong Polytechnic University, Hong Kong
enluchao@polyu.edu.hk

Phone: +44 (0)191 227 4902, Fax: +44 (0)191 227 3684

Abstract—The paper presents a new node architecture for an all-optical packet router employing multiple pulse position modulation (PPM) routing table with a hybrid packet header correlation scheme. Most existing routing tables within a node contain a large number of entries, thus resulting in a long packet header address correlation time before delivering the incoming packet to its destination. In the proposed multiple PPM routing tables (PPRTs) the packet header address is based on the binary and PPM formats which leads to a much reduced routing table size. The packet header address correlation is carried out using only a single optical AND gate, thus offering reduced system complexity. It is also shown that the proposed scheme offers unicast/multi-cast/broadcast transmitting capabilities. The propose scheme is simulated and its characteristics are investigated. The output inter-channel crosstalk (CT) of up to -18 dB and output packet power fluctuation of 2 dB have been achieved, which largely depend on the guard time between the arriving packets.

Index Terms— Packet switching, pulse position modulation, address modulation, address correlation, optical switch.

I. INTRODUCTION

In high-speed all-optical packet routing it is advantageous to replace packet header processing based on the slow optical/electrical/optical (O/E/O) conversion modules with an entirely optical scheme to achieve a higher data throughput and lower power consumption [1, 2]. In recent years we have seen the development of Boolean logic gates [3-5] (such as AND, OR and XOR) with the operating data rates higher than 40 Gbit/s have become the key enabling technology for realizing all-optical processing, data storing (flip-flop) and

packet routing. Common packet header processing is carried out by sequentially correlating the incoming packet header address with each entry of a local routing table. For a small size network this is viable provided the routing table size is small. However, for a large size network with a routing table with hundreds or thousands of entries, the cost, complexity and packet header processing become a real issue. In [6] it has been shown that packet header processing time (i.e. correlation time) can be significantly reduced by adopting a multiple PPM routing table where only a subset of the header address is converted into a PPM format. To generate a PPM format in each node will require a serial to parallel converter (SPC), an array of 1×2 optical switches, and fibre delay lines. However, to convert a long header address, a large number of optical switches and delay lines are required, thus resulting in deterioration of the extinction in the PPM-converted address [7].

In this paper, we propose a simple hybrid header address correlation scheme with no PPM address conversion module, offering a number of advantageous including (i) significantly reduced routing table entries, (ii) considerably reduced correlation processing time by using merely a single bitwise AND gate instead of a large number of gates with a low response-time, and (iii) unicast, multi-cast and broadcast transmission modes embedded in the optical layer. The proposed scheme offers reduced complexity compared with a previous correlation scheme due to exclusion of the PPM address conversion module [6]. The paper is organized as follows: after the introduction, the format of the hybrid header address and the principle of the multiple PPRTs are illustrated in Section 2. The proposed node architecture is outlined in Section 3. In Section 4 simulation results and discussions are presented. Finally, Section 5 will conclude the paper.

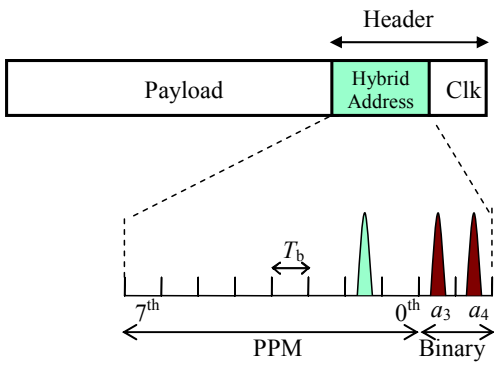


Fig. 1. An optical packet with a hybrid header address format equivalent to N -bit conventional address pattern ($N = 5$), T_b is the bit duration.

II. HYBRID HEADER ADDRESS CORRELATION

A. Hybrid Address

A typical packet is composed of a header (clock and address) and a payload. The clock signal, normally the first bit within the packet header, is used for synchronization within the router. In contrast to the conventional header address

format, which is binary, here we have adopted a hybrid binary and PPM formats. Here a packet composed of 3-element is defined by a set $S = \{S_C, S_A, S_P\}$, where the elements representing the clock, address, and payload, respectively is given as:

$$S_C = 1,$$

$S_A = \{S_{A1}, S_{A2}\}$, where S_{A1} and S_{A2} represent the most significant bits and a PPM format given as:

$$S_{A1} = \{a_{N-1}, a_{N-2}, \dots, a_{N-X}\}, \forall S_{A1} \in \{0, 1\}$$

$$S_{A2} = \{b_0, b_1, \dots, b_d, \dots, b_{(2^{N-X}-1)}\}, \exists b_d = 1 \text{ representing a PPM pulse and the rest of elements are equal to } "0", \text{ where the decimal value of the binary address bits is } d = \sum_{i=0}^{N-X-1} a_i \times 2^i,$$

N and X represent the conventional header length and its two MSBs, respectively

$$S_P = \{p_0, p_1, p_2, \dots, p_{l-1}\}, \forall S_P \in \{0, 1\}, \text{ where } l \text{ is the payload bit resolution.}$$

For example, an N -bit binary address $\{a_4 \ a_3 \ a_2 \ a_1 \ a_0\}$ of $\{11001\}$ in the hybrid format is “1101000000”, where the first two bits correspond to X and the remaining bits represent a PPM frame of length 2^{N-X} with a pulse located in position 2 corresponding to the decimal value of $\{a_2 \ a_1 \ a_0\}$, see Figure 1.

TABLE I
THE CONVERSION OF CONVENTIONAL RT TO SINGLE PPRT

Address patterns ($N=5$)	Output port	PPRT entries with 32 slots ($N=5$)
00000 00001 00011 00101 01001 01101 10000 10011 10101 11000 11100 11110	1	Decimal values 0 1 3 5 9 13 16 19 21 24 28 30 PPM pulses E_1
00000 00001 00010 00110 01010 01100 01111 10000 10111 11010 11101	2	Decimal values 0 1 2 6 10 12 15 18 23 26 29 PPM pulses E_2
00000 00100 00111 01000 01011 01110 10001 10100 10110 11001 11011 11111	3	Decimal values 0 4 7 8 11 14 17 20 22 25 27 31 PPM pulses E_3

TABLE II
THE CONVERSION OF CONVENTIONAL RT TO MULTIPLE PPRTS

Address patterns ($N=5$)	PPRT entry	4 Multiple PPRT entries with 8 slots ($N=5, X=2$)
$E_{1D} \left\{ \begin{array}{l} 00000 \\ 00001 \\ 00011 \\ 00101 \\ 01001 \\ 01101 \end{array} \right.$	E_1	0 1 3 5 9 13 16 19 21 24 28 30 E_1
$E_{1C} \left\{ \begin{array}{l} 00101 \\ 01001 \\ 01101 \\ 10000 \\ 10011 \\ 10101 \\ 11000 \\ 11100 \\ 11110 \end{array} \right.$		 E_{1C}
$E_{1B} \left\{ \begin{array}{l} 10000 \\ 10011 \\ 10101 \\ 11000 \\ 11100 \\ 11110 \end{array} \right.$		 E_{1B}
$E_{1A} \left\{ \begin{array}{l} 11110 \end{array} \right.$		 E_{1A}
$E_{2D} \left\{ \begin{array}{l} 00000 \\ 00001 \\ 00010 \\ 00110 \\ 01010 \\ 01100 \\ 01111 \\ 10000 \\ 10111 \\ 11010 \\ 11101 \end{array} \right.$	E_2	0 1 2 6 10 12 15 18 23 26 29 E_2
$E_{2C} \left\{ \begin{array}{l} 00110 \\ 01010 \\ 01100 \\ 01111 \\ 10010 \\ 10111 \\ 11010 \\ 11101 \end{array} \right.$		 E_{2C}
$E_{2B} \left\{ \begin{array}{l} 10010 \\ 10111 \\ 11010 \\ 11101 \end{array} \right.$		 E_{2B}
$E_{2A} \left\{ \begin{array}{l} 11101 \end{array} \right.$		 E_{2A}
$E_{3D} \left\{ \begin{array}{l} 00000 \\ 00100 \\ 00111 \\ 01000 \\ 01011 \\ 01110 \\ 10001 \\ 10100 \\ 10110 \\ 11001 \\ 11011 \\ 11111 \end{array} \right.$	E_3	0 1 2 6 10 12 15 18 23 26 29 E_3
$E_{3C} \left\{ \begin{array}{l} 00110 \\ 01011 \\ 01110 \\ 10001 \\ 10100 \\ 10110 \\ 11001 \\ 11011 \\ 11111 \end{array} \right.$		 E_{3C}
$E_{3B} \left\{ \begin{array}{l} 10001 \\ 10100 \\ 10110 \\ 11001 \\ 11011 \\ 11111 \end{array} \right.$		 E_{3B}
$E_{3A} \left\{ \begin{array}{l} 11111 \end{array} \right.$		 E_{3A}

B. Multiple Pulse Position Routing Tables

For a packet with N -bit header address $\{a_{N-1} a_{N-2} \dots a_2 a_1 a_0\}$, where a_{N-1} is the most significant bit (MSB), the conventional routing table (RT) will have a maximum of 2^N entries. In the worst case scenario i.e. checking all entries, the router will perform 2^N N -bitwise correlations. Table I illustrates a routing table for $N = 5$ and its equivalent PPM versions. For each output of the node, there exists a single PPRT entry with 2^N slots. In this example, the standard PPRT has three entries E_i ($i = 1, 2, 3$) of length 32 slots with duration T_s . Here T_s is set to be equal to the bit duration T_b of 6.25 ps. The locations of the short pulses in each entry correspond to the decimal values of conventional binary address patterns in i^{th} group. In multiple PPRTs, entry length could be reduced from $32T_s$ to $2^{N-X}T_s$ by splitting each PPRT entry into sub-groups of E_{ij} ($i = 1, 2, 3$, and $j = A, B, C, D$), see Table II. A, B, C and D represent address patterns with decimal metrics in ranges of (24-31), (16-23), (8-15) and (0-7), respectively. For $X = 2$ and $N = 5$ the PPRT entry length is reduced from $32T_s$ to $8T_s$.

III. NODES ARCHITECTURE

The proposed router with a multiple PPRT and M -output

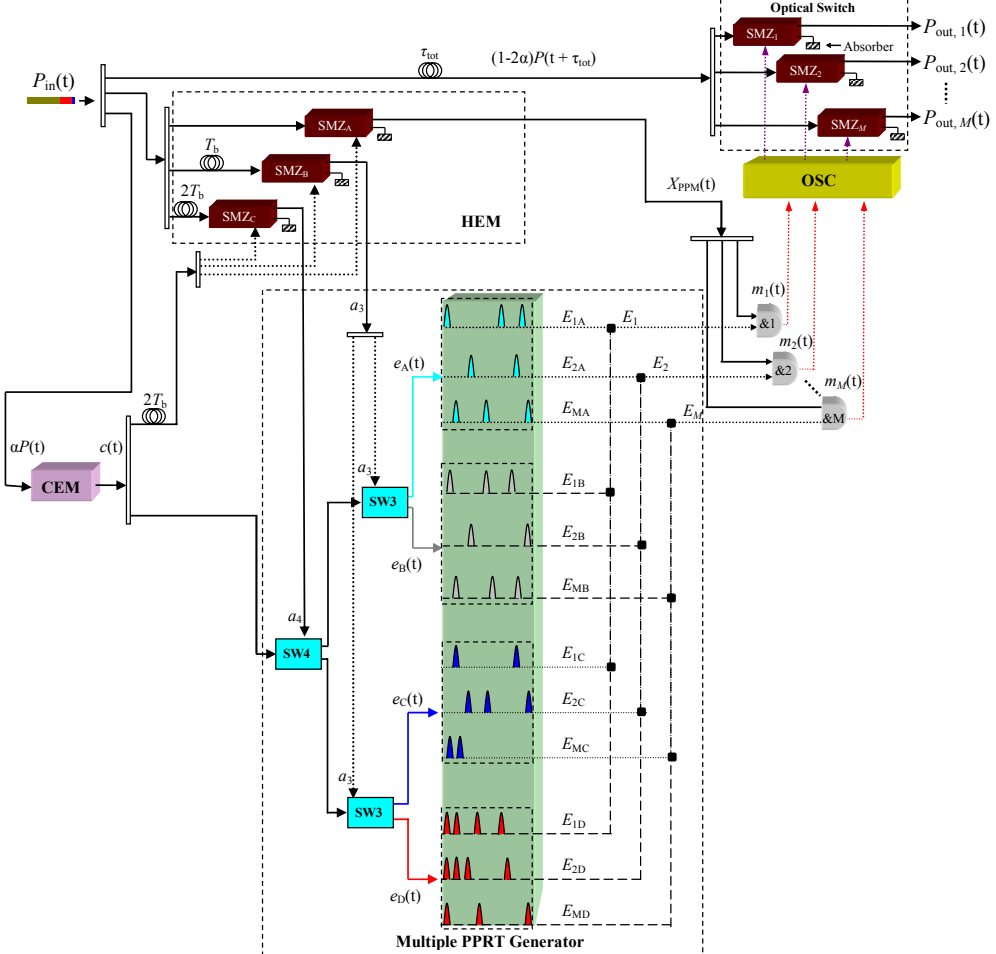


Fig. 2. The node architecture for packets with hybrid header address (where $N=5, X=2$).

ports is composed of a number of main modules including a clock extraction module (CEM), a header address extraction module (HEM), a multiple PPRT generator, AND gates, $1 \times M$ all-optical switch, an optical switch control module (OSC), and a number of 1×2 high extinction ratio optical switches (SW) [7], see Figure 2. The received packet $P_{in}(t)$ after splitting is applied to the CEM, HEM and optical switch modules, respectively. The extracted clock pulse $c(t)$ having been delayed by $2T_b$ and 0 is applied to the HEM and SW4, respectively, whereas the outputs of HEM are applied to the SWs 3&4 and the AND gates. The two MSB bits (a_4 and a_3) are checked by SWs 4&3 to select the first two groups E_A and E_B , and E_C or E_D of multiple PPRTs, respectively for address correlation. PPRTs with the same i^{th} index are combined together and applied to the optical AND gates for address correlation. Note that, only one multiple PPRT is used for correlation with an incoming packet header address $X_{PPM}(t)$. The outputs of the multiple PPRTs, see Figures 2, are given as [6]:

$$E_k(t) = E_{kA}(t) + E_{kB}(t) + E_{kC}(t) + E_{kD}(t). \quad (1)$$

Where each d_k element corresponds to the decimal values of the header address bits assigned to the node output k^{th} ($k = 1, 2, \dots, M$).

The SMZ based optical AND gates [7] outputs are given by:

$$m_k(t) = X_{PPM}(t) \times E_k(t) = \begin{cases} 1 & \text{if } d_k = \sum_{i=0}^{N-1} a_i \times 2^i \quad \forall k \\ 0 & \text{if } d_k \neq \sum_{i=0}^{N-1} a_i \times 2^i \quad \forall k \end{cases},$$

$k = 1, 2, \dots, M \quad d_k \in \{0 \sim (2^N - 1)\}$. (2)

$m_k(t)$ are applied to the OSC module to ensure that incoming packets $P_{in}(t)$ delayed by τ_{tot} (total required time for header

address correlation) are switched to the correct output ports. The switched packet is given as:

$$P_{out,k}(t) = P_{in}(t) \times m_k(t) = \begin{cases} G_{OS} \times (1 - 2\alpha) \times P_{in}(t + \tau_{tot}) & \text{if } m_k(t) = 1 \\ 0 & \text{if } m_k(t) = 0 \end{cases} \quad k = 1, 2, \dots, M$$
(3)

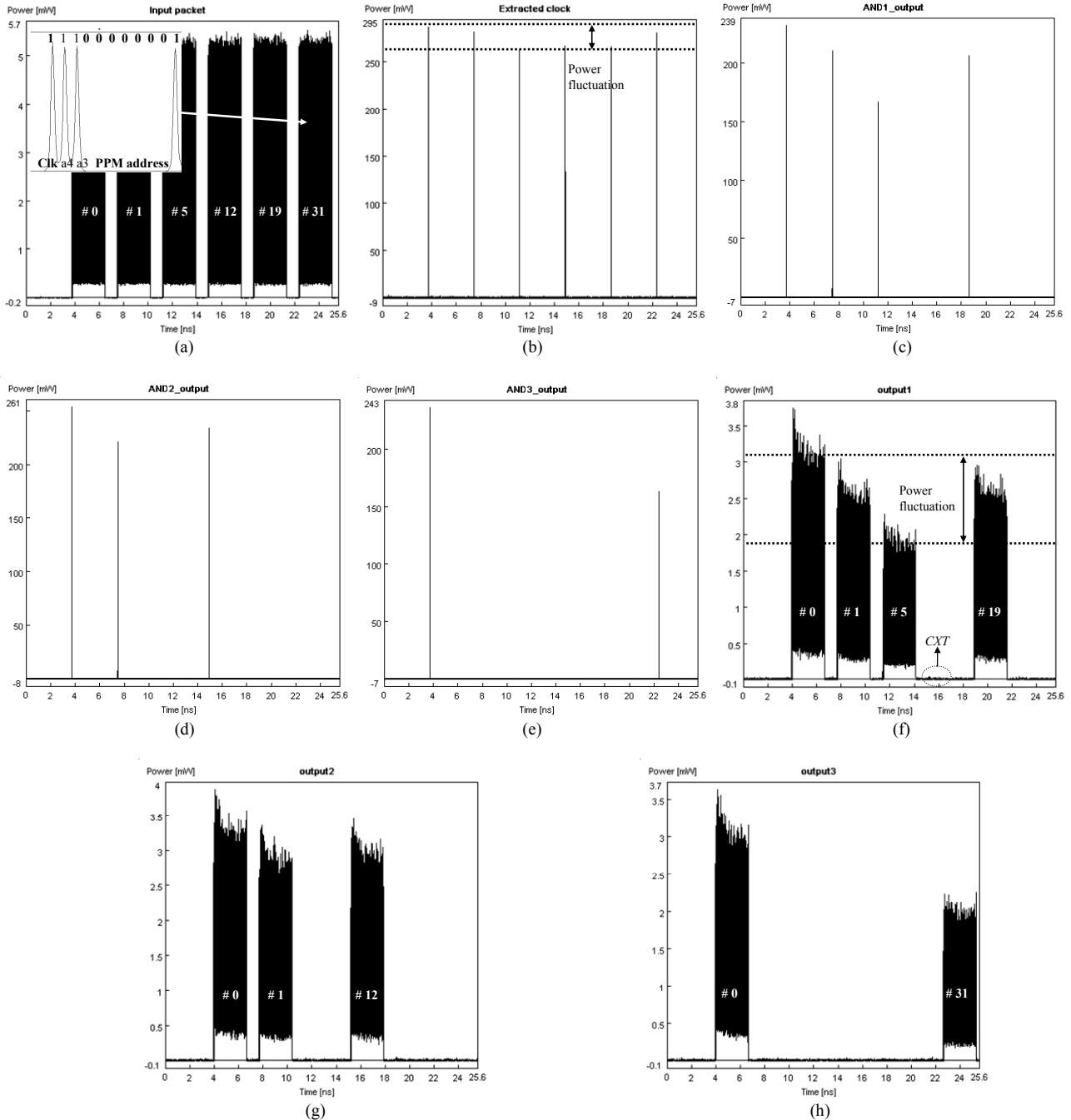


Fig. 3. Time waveforms of (a) input packets, (b) extracted clock signals, (c) matched signals at AND gate 1, (d) matched signals at AND gate 2, (e) matched signals at AND gate 3, (f) switched packets at router's output 1, (g) switched packets at router's output 2, and (h) switched packets at router's output 3.

TABLE III
SIMULATION PARAMETERS

Parameter and description	Value
Data packet bit rate – $1/T_b$	160 Gb/s
Packet payload length	53 bytes (424 bits)
Wavelength of data packet	1552.52 nm (193.1 THz)
Data pulse width – FWHM	2 ps
PPM slot duration $T_s (=T_b)$	6.25 ps
Average transmitted power P_{in}	5 mW
Average power of $C_d(t)$	270 mW
Optical bandwidth	300 GHz
Splitting factor α	0.2
Inject current to SOA	150 mA
SOA length	500 μ m
SOA width	3×10^{-6} m
SOA height	80×10^{-9} m
SOA n_{sp}	2
Confinement factor	0.15
Enhancement factor	5
Differential gain	2.78×10^{-20} m ²
Internal loss	40×10^2 m ⁻¹
Recombination constant A	1.43×10^8 s ⁻¹
Recombination constant B	1.0×10^{-16} m ³ s ⁻¹
Recombination constant C	3.0×10^{-41} m ⁶ s ⁻¹
Carrier density transparency	1.4×10^{24} m ⁻³
Initial carrier density	3×10^{24} m ⁻³

where G_{OS} is the optical switch gain.

If more than one pulse is located at the same position in more than one (or all) PPRT entries, then the packet is broadcasted to multiple outputs (i.e. multicast) or all outputs (i.e. broadcast), respectively.

IV. RESULTS AND DISCUSSIONS

The router shown in Figure 2 is simulated using the Virtual Photonics simulation software (VPITM). By taking advantage of the hybrid address, the new node architecture could be constructed with reduced complexity due to exclusion of the PPM address conversion module within the router. Table III shows all the main simulation parameters adopted [7]. Six optical packets with addresses of #0, #1, #5, #12, #19 and #31 (decimal values) are transmitted sequentially at 160 Gb/s with 1 ns inter-packet guard time. Each packet contains a 1-bit clock, a 10-bit hybrid address and a 53-byte payload (ATM cell size) [8]. Figure 3(a) shows the time waveforms of the six input packets with the inset illustrating the zoomed-in packet hybrid header with an address decimal metric of #31. The extracted clock pulses are presented in Figure 3(b). Figures 3(c), 3(d), and 3(e) illustrate the time waveforms observed at the outputs of AND gates 1, 2, and 3, respectively. Time waveforms of signals at the output ports 1, 2, and 3 of the router are depicted in Figures 3(f), 3(g), and 3(h), respectively, confirming that the incoming packets with header addresses of #0, #1, #5, #12, #19 and #31 are switched to outputs 1 & 2, 1, 2, 1, and 3, respectively, based on the

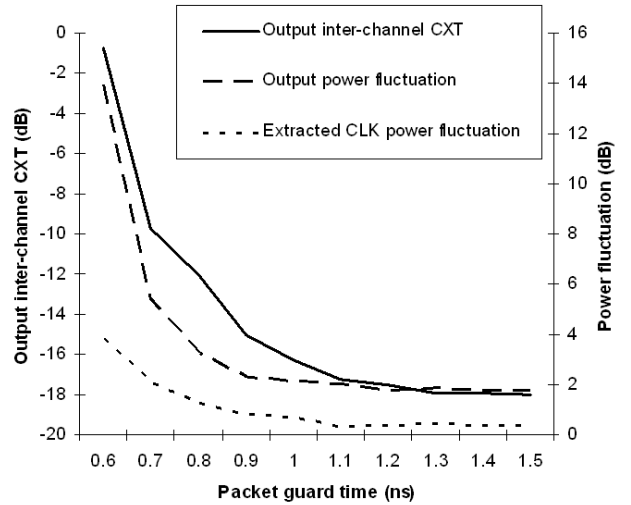


Fig. 4. Packet guard time against the output inter-channel CXT (left x-axis), output packet power fluctuation (right x-axis) and the extracted clock power fluctuation (right x-axis).

routing information given in Tables I and II. In addition, unicast, multicast and broadcast transmitting capabilities of the router are also demonstrated as packets with addresses of #5, #12, #19, and #31 are switched to one output port of the router, whereas the packets with #1 and #0 addresses are switched to two and all output ports of the router, respectively. Figure 4 investigates the output inter-channel CXT and power fluctuation against the different packet guard time observed at the output 1. The CXT is defined as:

$$CXT = 10 \log_{10} (P_{nt} / P_t) \quad (4)$$

where P_{nt} is the peak output signal power of the undesired packet and P_t is the average output signal power of the lowest target desired packet. The undesired CXT is due to the incompletely cut-off edge of the switching window profile induced by the slow gain recovery of the SOA [9]. CXT is high for lower values of the packet guard time, improving significantly by increasing the guard time reaching ~ 18 dB beyond the packet guard time of 1.2 ns. This improvement is due to the switching window being completely closed. However as the guard time increases beyond 1.2 ns, no further improvement is achieved. This is because the CXT is solely due to the extinction ratio of matched signal $m(t)$, see Figure 2.

The power fluctuation of the extracted clock signals and the output packets are defined by the differences between the highest and lowest intensity in decibel, see Figure 3(b) and 3(f), respectively. Figure 4 shows that the minimum power fluctuations of the clock signal and the output packets are 0.3 dB and 2 dB, respectively. The observed power fluctuation of the switched packets is mainly due to the unequal output power of the AND gates, see Figure 3(c)-(e). This is because power fluctuation of the extracted clock signals (see Figure 3(b)) increases after passing through two amplification stages (i.e. SW4 and SW3), thus resulting in an unequal input power at the input of the AND gates. Thus the need for a wider packet guard time of greater than 1 ns.

V. CONCLUSION

The paper has presented an all-optical packet-switched routing scheme with a hybrid header address correlation scheme. The $1 \times M$ router architecture with the multiple PPRTs is also illustrated, the proposed routing scheme offers a reduced complexity and avoids the speed limitation imposed by the non-linear element based optical AND gates. Header processing and packet routing have been simulated and the results obtained show that this router can operate at 160 Gb/s with the output inter-channel crosstalk (*CXT*) of up to -18 dB and the margin of output packet power fluctuation is 2 dB largely dependent on the guard time between the packets.

REFERENCES

- [1] G. K. Chang, J. Yu, Y. K. Yeo, A. Chowdhury, Z. S. Jia, "Enabling technologies for next-generation optical packet-switching networks," *Proceedings of IEEE*, vol. 94, no. 5, pp. 892-910, 2006.
- [2] E. T. Y. Liu, Z. Li, S. Zhang, M. T. Hill, J. H. C. van Zantvoort, F. M. Huijskens, H. de Waardt, M. K. Smit, A. M. J. Koonen, G. D. Khoe, and H. J. S. Dorren, "Ultra-fast all-optical signal processing: toward optical packet switching," *Proceedings of SPIE*, vol. 6353, pp. 635312-1 - 635312-12, 2006.
- [3] Z. Li and G. Li, "Ultrahigh-speed reconfigurable logic gates based on four-wave mixing in a semiconductor optical amplifier," *IEEE Phot. Tech. Lett.*, vol. 18, no. 12, pp. 1341-1343, 2006.
- [4] H. Dong, H. Sun, Q. Wang, N. K. Dutta, and J. Jaques, "All-optical logic and operation at 80 Gb/s using semiconductor optical amplifier based on the Mach-Zehnder interferometer," *Micro. & Opti. Tech. Lett.*, vol. 48, no. 8, pp. 1672-1675, 2006.
- [5] H. Sun, Q. Wang, H. Dong, Z. Chen, N. K. Dutta, J. Jaques, and A. B. Piccirilli, "All-optical logic XOR gate at 80 Gb/s using SOA-MZI-DI," *IEEE J. Quantum Electron.*, vol. 42, no. 8, pp. 747-751, 2006.
- [6] M. F. Chiang, Z. Ghassemlooy, W. P. Ng., and H. Le-Minh: "Ultra-fast all-optical packet-switched router with multiple pulse position routing tables", *Proc the 12th European Conference on Networks & Optical Communications (NOC 2007)*, Kista Stockholm, Sweden, pp. 571-578, Jun. 2007.
- [7] H. Le-Minh, Z. Ghassemlooy, and W. P. Ng., "Multiple-hop routing based on the pulse-position modulation header processing scheme in all-optical ultrafast packet switching network," *Proc GLOBECOM 2006*, San Francisco, USA, Nov. 2006.
- [8] L. Angrisani, A. Baccigalupi, and G. D'Angiolo, "A frame-level measurement apparatus for performance testing of ATM equipment," *Instrumentation and Measurement, IEEE Transactions*, vol. 52, no. 1, pp. 20-26, 2003.
- [9] H. Le-Minh, Z. Ghassemlooy, and W. P. Ng, "Investigation of control pulse power effects on all-optical SMZ switch performance", *Proc the 5th International Symposium on Communication Systems, Networks and Digital Signal Processing (CSNDSP 2006)*, Patras, Greece, pp. 449-453, Jul. 2006.